First ICN Adduct with a Selenium Donor (R = Se): Is It an Ionic $[RSeCN]^+I^-$ or a "T-Shaped" R(I)SeCN Hypervalent Compound?

M. Carla Aragoni,[a] Massimiliano Arca,[a] Francesco Demartin,[b] Francesco A. Devillanova,*[a] Alessandra Garau,[a] Patrizio Grimaldi,[c] Francesco Isaia,[a] Francesco Lelj,[c] Vito Lippolis,[a] and Gaetano Verani[a]

Keywords: Density functional calculations / Donor-acceptor systems / ICN / Hypervalent compounds / Se ligands

The reaction between 1,3-dimethyl-4-imidazoline-2-selone (**2**) and ICN gave the adduct **2**·ICN, whose crystal structure features dimers made up of two $[\mathbf{2}\cdot CN]^+$ and two I^- which strongly interact. Hybrid DFT calculations on the adduct **2**·ICN, on the cation $[\mathbf{2}\cdot CN]^+$, and on the dimer $(\mathbf{2}\cdot ICN)_2$ account for a partially hypervalent selenium atom in **2**·ICN and for the observed structural features.

Introduction

Hypervalent chalcogen compounds featuring a linear X−E−X moiety (X = Cl, Br, I; E = S, Se) can be considered to derive from the oxidative addition of an X_2 molecule to a donor molecule containing the chalcogen atom. With donors containing thio- or seleno-carbonyl groups, the "T-shaped" nature of the corresponding adducts is well explained by the VSEPR model,[1] according to which the geometry at the chalcogen atom is a pseudo-trigonal bipyramid (tbp) with the halogens occupying the apical positions. These compounds are commonly reported as 10−E−3 systems,[2] indicating that the chalcogen atom E is formally associated with five electron pairs (10 electrons), only 3 of which are bond pairs. As with a tri-halide, the chemical bond in the linear X−E−X fragment has also been described as a three-center−four-electron (3c-4e) system, whose simplified MO diagram can be built by combining the p_z atomic orbitals of the central chalcogen and those of the two terminal halogen atoms.[3] Four electrons occupy only the bonding and non-bonding orbitals, thus determining a total bond order of 1 (0.5 for each E−X bond). This description agrees with the qualitative observation[4,5] that on increasing the electronegativity difference between the halogen and the chalcogen, hypervalent chalcogen adducts are formed more easily than charge-transfer (CT) adducts bearing the E−X−X linear group (10−X−2 hypervalent halogen compounds).[2] Indeed, the number of hypervalent sulfur and selenium compounds structurally characterized decreases on passing from chlorine to iodine, and hypervalent sulfur compounds with di-iodine are unknown.[6] In addition, the first hypervalent selenium compounds with iodine were only reported in 1994,[7,8] and the first hypervalent sulfur compound with bromine appeared in 1977,[9] and the second in 1999.[10]

For the oxidative addition of inter-halogens (ICl, IBr), only two examples of "T-shaped" adducts have been reported, i.e. **1**·IBr,[9] which is very unstable, and **3**·2IBr.[11] In addition, **1**·BrCN (characterized by X-ray diffraction)[9] and **1**·ClCN (characterized only by IR spectroscopy)[9] are the only reported examples of S- or Se-adducts with pseudohalogens (ICN, BrCN, and ClCN). Therefore, the synthesis of new such adducts is an important step towards understanding not only the nature of the chemical bond in these systems, but also the possible role of hypervalent chalcogen compounds as intermediates in the formation of the many classes of compounds obtained by reacting chalcogen donors with halogens and inter-halogens.[6,12,13]

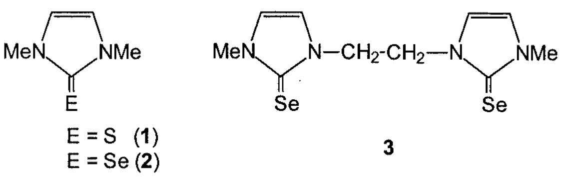

---

[a] Dipartimento di Chimica Inorganica ed Analitica, Università di Cagliari, Cittadella Universitaria,
09042 Monserrato-Cagliari, Italy
Fax: (internat.) + 39-070-6754456
E-mail:devilla@unica.it

[b] Dipartimento di Chimica Strutturale e Stereochimica Inorganica e Centro CNR, Università di Milano,
Via G. Venezian 21, 20133 Milano, Italy

[c] LAMI Dipartimento di Chimica and LASCAMM-INSTM Sezione Basilicata, Università della Basilicata,
Via N. Sauro, 85100 Potenza, Italy

DOI: 10.1002/ejic.200300762

This paper contributes to this chemistry by reporting both the crystal structure of the first selenium adduct with the pseudo-halogen ICN and the DFT calculations that have been of great help in ascertaining the nature of the chemical bond in the ISeCN fragment.

Results and Discussion

Synthesis and Structural Characterization: The reaction of **2** with one equivalent of ICN in CH$_2$Cl$_2$ gave well-shaped crystals by slow evaporation of the solvent. X-Ray diffraction analysis showed that the asymmetric unit is formed by the adduct 2·ICN bearing the I···Se−CN linear group [I···Se−C(8) 174.8(2)°] almost perpendicular to the imidazolidine ring, with a very long Se···I distance [3.300(1) Å] and a short Se−CN bond [1.885(5) Å]. Two 2·ICN units are arranged about a crystallographic inversion center to form dimers via Se···I contacts that are only 0.117 Å longer than the Se···I distance within the asymmetric unit (Figure 1), so that the two selenium and two iodine atoms are located on the opposite corners of an almost regular rhombus. The very long Se···I distances suggest the isolated compound has an ionic nature.

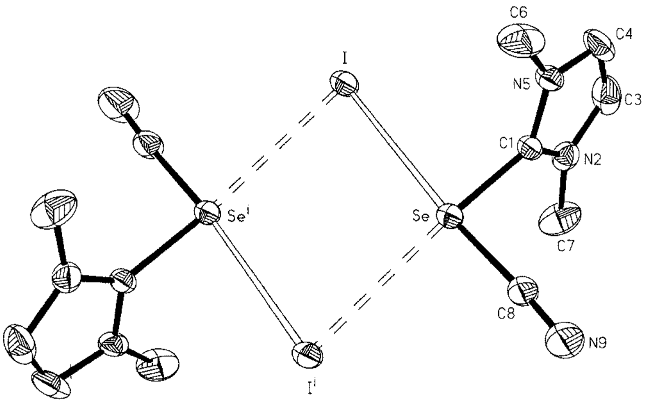

Figure 1. Molecular structure and atom labelling scheme for the adduct **2**·ICN; selected bond lengths and angles: Se···I 3.300(1), Se···I^i 3.417(1), C(1)−Se 1.913(4), C(8)−Se 1.885(5)Å, C(1)−Se−C(8) 93.2(2), I···Se−C(8) 174.8(2), Se···I···Se^i 80.24(1), I···Se···I^i 99.76(1), N(2)−C(1)−Se−C(8) 83.2(4)°; i = − *x*, 1 − *y*, 1 − *z*

The structural features of **2**·ICN can usefully be compared with those of **1**·BrCN, the only other reported adduct between an S- or Se-donor and a pseudo-halogen.[9] According to the very long S···Br bond length, the authors described **1**·BrCN as an ion pair [**1**·CN]$^+$ Br$^-$. However, a dimeric arrangement similar to that observed for **2**·ICN can also be envisaged for **1**·BrCN, with two significantly different S···Br distances (3.270 and 3.587 Å). The S···Br involving the Br atom *trans* to the cyano group is the longest, contrary to what is observed in the dimer (**2**·ICN)$_2$. Intriguingly, the S···Br and Se···I distances *trans* to the cyano group in the two compounds are very similar, although the involved atoms are S and Br in **1**·BrCN and their heavier congeners, Se and I, in **2**·ICN. Thus, **2**·ICN might not be a pure ionic compound, and a partial selenium−iodine covalent character should be considered to fully explain the compound's structural features.

DFT Calculations: A partial covalent character for the Se···I bond in **2**·ICN would agree with a description for it as a strongly polarized hypervalent-selenium compound. Actually, the linearity of the I···Se−CN group supports this view, although this is not direct evidence for hypervalency of the selenium atom. Recently, we reported the crystal structure of **3**·2IBr, which was the first example of a hypervalent selenium compound with IBr. In **3**·2IBr, the two I−Se···Br systems were strongly polarized, both Se···Br bonds having, therefore, a partial ionic character.[11]

DFT calculations have greatly enabled deeper insight into the nature of the chemical bond in some CT and tbp adducts between halogens or inter-halogens and some S- or Se-donors, including **2**.[11,12] In particular, for **2**·I$_2$,[12] **2**·Br$_2$,[12] and **2**·IBr,[11] the calculated geometries of the organic frameworks are in very good agreement with the experimental data for **2**·I$_2$,[7] **3**·2I$_2$,[7] **3**·2Br$_2$,[14] and **3**·2IBr,[11] though in general the Se−X bond lengths were slightly overestimated. Hence, we performed calculations at the same level of theory on **2**·ICN (both in the tbp and in the CT type arrangements), on the dimer (**2**·ICN)$_2$ and on the [**2**·CN]$^+$ cation. Interestingly, the optimized geometry for the tbp **2**·ICN adduct agrees fairly well with the structural data (Figure 2) with the exception of the Se···I length, which is underestimated (3.233 Å) as compared with the experimental value [3.300(1) Å]. The structural features of the organic framework for the optimized geometry of (**2**·ICN)$_2$ are very similar to those of the calculated geometry of **2**·ICN (Figure 2). The Se···I distances are calculated to be slightly dissimilar (3.448 and 3.422 Å, respectively) as ex-

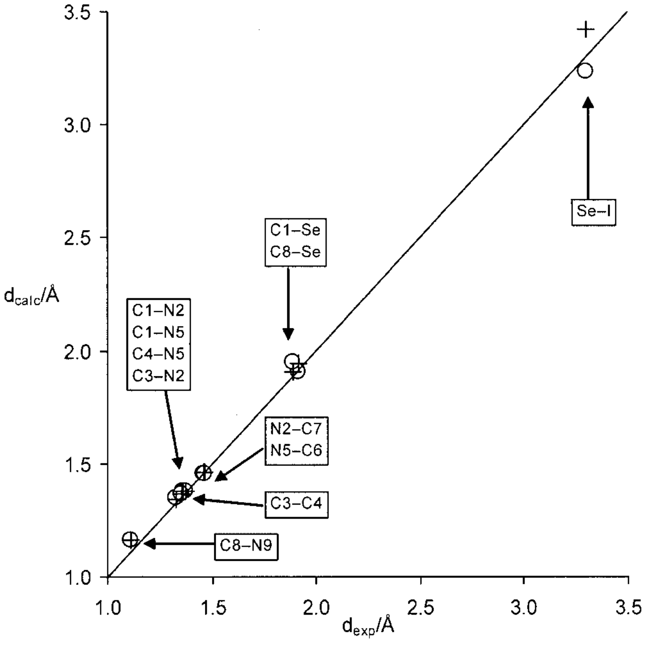

Figure 2. Correlation between the experimental (d_{exp}) bond lengths for **2**·ICN and the optimized (d_{calc}) ones for **2**·ICN (O) and (**2**·ICN)$_2$ (+)

perimentally found, but overestimated with respect to the experimental data [Se···I$^{\mathrm{i}}$, 3.417(1); Se···I, 3.300(1) Å, Figure 1].

Previously,[11,12] we proved by DFT calculations that the complete removal of one of the two halogen atoms as a halide from an X−Se−X (X = I, Br) hypervalent system (the two extremes being the covalent and completely ionic bonds) causes the carbon−selenium−halogen angle to open from lower than 90° towards values closer that expected for a tetrahedral environment around the chalcogen atom. For example, the calculated C−Se−X (X = I, Br) angles pass from 84.3° for the "T-shaped" **2**·Br_2 adduct to 97.2° for the cation $[\mathbf{2}\cdot\mathrm{Br}]^+$, and from 85.4° for the analogous **2**·I_2 adduct to 98.3° for $[\mathbf{2}\cdot\mathrm{I}]^+$.[11,12] The widening of the C−Se−X angle represents the most significant change observed in the optimized structural parameters upon lengthening of one Se−X bond of the hypervalent system towards the formation of the $[>\mathrm{C{-}Se{-}X}]^+$ cation; all the other structural features are only slightly changed. In the present case, the calculated C−Se−CN angle shows a very small variation (91.8° in **2**·ICN; 94.7° in $[\mathbf{2}\cdot\mathrm{CN}]^+$; Table 1). This small variation is justified as the optimized geometry for the "T-shaped" **2**·ICN adduct already shows a very strong polarization of the Se···I bond determined by the very different electronic effects of the I and CN groups bonded to the Se atom. This is also indicated by the calculated NBO[15,16] charges on the iodine atom, which are −0.665 and −0.718e for **2**·ICN and $(\mathbf{2}\cdot\mathrm{ICN})_2$ respectively. Therefore, the increase in the negative charge on the iodine atom up to the limit case of −1 in $[\mathbf{2}\cdot\mathrm{CN}]^+$ does not change significantly the structural features of the organic framework including the C−Se−CN angle. Interestingly, the experimental C−Se−CN angle [93.2(2)°] is exactly in between those calculated for the tbp **2**·ICN adduct and the cation $[\mathbf{2}\cdot\mathrm{CN}]^+$. A similar situation is observed for **1**·BrCN:[9] the experimental C−S−CN angle of 96.3° is slightly lower than the 98.5° calculated for the cation $[\mathbf{1}\cdot\mathrm{CN}]^+$ (footnote [c] in Table 1) and very close to the 96.5° calculated for the tbp **1**·BrCN adduct.

Table 1. Selected bond lengths, angles, and NBO charges for the optimized geometries of "T-shaped" adducts between **2** and XY (X = Y = Cl, Br, I; X = I and Y = Cl, Br, CN), calculated at the DFT level

X Y	Cl[a] Cl	Br[b] Br	I[a] I	I[a] Br	I[a] Cl	I[a][c] CN	I[a,c] CN dimer
d(C−Se)/Å	1.894	1.870	1.890	1.891	1.891	1.905	1.910
d(Se−X)/Å	2.588	2.602	2.983	2.964	2.953	3.233	3.422
d(Se−Y)/Å	2.588	2.602	2.983	2.794	2.619	1.952	1.945
X−Se−C/deg	84.8	84.3	85.4	86.5	87.2	71.8	71.2
Y−Se−C/deg	84.8	84.3	85.4	83.8	82.8	91.8	90.7
Q_X/e	−0.488	−0.449	−0.393	−0.387	−0.392	−0.665	−0.718
Q_Y/e	−0.488	−0.449	−0.393	−0.447	−0.486	−0.378	−0.342
Q_{Se}/e	0.403	0.354	0.212	0.259	0.305	0.472	0.488
Q_C/e	0.280	0.220	0.271	0.275	0.276	0.271	0.280

[a] LANL2DZ basis set for halogen atoms. [b] 6−31 g** Basis set for halogen atoms. [c] Values for the $[\mathbf{2}\cdot\mathrm{CN}]^+$ cation: *d*(C−Se) 1.918, *d*(Se−CN) 1.861 Å, ∠C−Se−CN 94.7°, Q_{Se} +0.532, Q_{CN} −0.251 e; for $[\mathbf{1}\cdot\mathrm{CN}]^+$, *d*(C−S) 1.768, *d*(S−CN) 1.712 Å, ∠C−S−CN 98.5°, Q_S +0.366, Q_{CN} −0.177 e.

In any event, the greater the difference in the electron-withdrawing features of the two groups interacting with the chalcogen atom, the lower is the covalency of the system X−Se−Y, which tends to become more polarized and ionic in nature.

In fact, the C−Se−I angle calculated for the tbp **2**·IBr adduct and the cation $[\mathbf{2}\cdot\mathrm{I}]^+$ are 86.5 and 98.3°, respectively;[11] the same angles observed for the two I−Se−Br units in the crystal structure of **3**·2IBr are 95.6(3)° and 90.6(3)°, in agreement with the different degree of covalency and hypervalency in the two systems.[11]

Partial hypervalency of the selenium atom in **2**·ICN is also supported by analysis of the LUMO and the LUMO+1 calculated for both cations $[\mathbf{1}\cdot\mathrm{CN}]^+$ and $[\mathbf{2}\cdot\mathrm{CN}]^+$. In fact, they are σ* and π* in nature with respect to the Se−C−N vector and very close in energy and symmetry-allowed to accept charge density either from donor halides *trans* to the cyano group (LUMO) or *trans* to the imidazoline ring (LUMO+1) (Figure 3). Thus, the formation of $(\mathbf{2}\cdot\mathrm{ICN})_2$ could be described as a charge-transfer interaction between the HOMOs of two I^- and the LUMO and LUMO+1 of two cations $[\mathbf{2}\cdot\mathrm{CN}]^+$. The closeness in energy of LUMO and LUMO+1 tends to make the interactions in the two directions equally likely, and solid-state

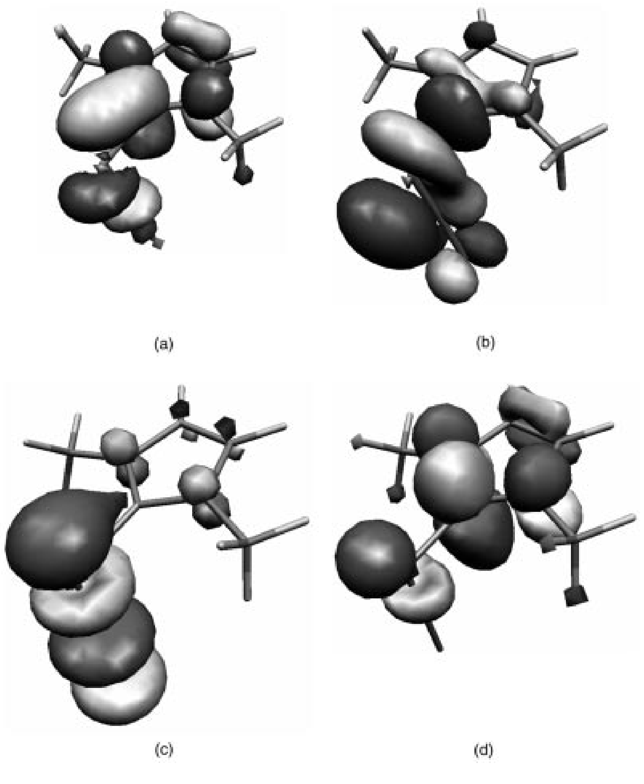

Figure 3. DFT LUMOs and (LUMO+1)s calculated for $[\mathbf{2}\cdot\mathrm{CN}]^+$ (a and b, respectively) and $[\mathbf{2}\cdot\mathrm{I}]^+$ (c and d, respectively); the calculated KS-orbital energies are −0.2222 (a), −0.1969 (b), −0.2902 (c), and −0.1853 (d) hartree; the corresponding molecular orbitals calculated for $[\mathbf{2}\cdot\mathrm{Br}]^+$, $[\mathbf{1}\cdot\mathrm{CN}]^+$, and $[\mathbf{1}\cdot\mathrm{I}]^+$ show similar compositions

effects might presumably be crucial in determining the balance between the entities of the two interactions. NBO population analysis shows that the two generated hybrid atomic orbitals of I^- (1.89 and 1.83e) have a direction suitable to put electron charge on LUMO and LUMO+1. The NBO population suggests that the amount of electron transfer is very low, but it should be important to determine the geometrical arrangement of the two **2**·ICN units in (**2**·ICN)$_2$. Conversely, for the hypervalent adducts with halogens and interhalogens, analysis of the LUMOs and (LUMO+1)s of the cations [**2**·X]$^+$ (X = I, Br; Figure 3) shows that both orbitals are σ^* in nature with respect to the Se−X vector and considerably separated in energy. Therefore, the donor−acceptor interaction between the lone pair of a halide Y^- (Y = I, Br) and the LUMO of the cation [**2**·X]$^+$ is the only one possible, giving a linear X−Se−Y moiety. This explains why, in hypervalent-chalcogen compounds with halogens,[6,12] the chalcogen−halogen bonds within the hypervalent systems are always considerably shorter than the chalcogen···halogen intermolecular contacts between adjacent adduct molecules. Thus, the topological analysis of the LUMO and LUMO+1 and the charge distribution seem to give both a decisive proof that the description of **2**·ICN as a polarized hypervalent-selenium compound is realistic and a good explanation for the different arrangements of the adduct units found in **1**·BrCN and **2**·ICN with respect to those observed for hypervalent-chalcogen systems with halogens and interhalogens.

Notably, a partial hypervalent nature of the Se atom in **2**·ICN does not imply a description of the Se···I bond as covalent, since DFT calculations indicate that this bond is strongly polarized and therefore appreciably ionic. However, comparison of the Se···I distances calculated both for **2**·ICN and (**2**·ICN)$_2$ with those of hypervalent adducts of **2** containing the Se−I bond (Table 1) and the trend of the calculated NBO[15,16] charge on the iodine atom of the I−Se−X system on passing from X = I to Br, Cl, and CN (Figure 4; Table 1) shows that **2**·ICN and (**2**·ICN)$_2$ are different from the other systems. The considerably long Se−I distances and the strongly negative charge on iodine [−0.665 and −0.718e in **2**·ICN and (**2**·ICN)$_2$ respectively][16] agree with the strongly polarized character of the Se···I bond in the present compound.

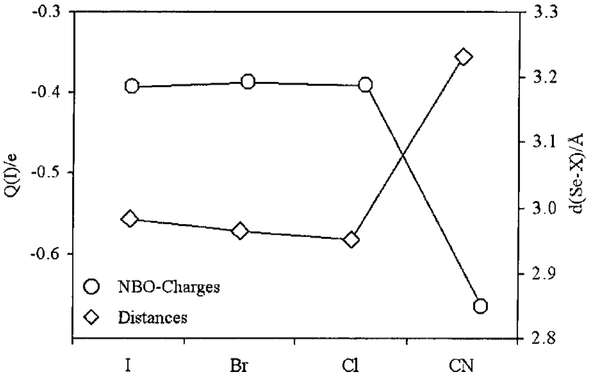

Figure 4. Trends of Se−I bond lengths and calculated NBO charge on the iodine atom for the I−Se−X system in **2**·IX T-shaped adducts (X = I, Br, Cl, CN)

We have also examined the relative energy of (**2**·ICN)$_2$ with respect to **2**·ICN and the starting reagents **2** and ICN. DFT-calculated energies show that, neglecting solvation effects and BSSE corrections, the **2**·ICN adducts of both the CT and the T-shaped types are unstable by 1.95 and 4.39 kcal mol^{-1}, respectively, compared with the free components **2** and ICN (Figure 5). Though slightly unstable with respect to **2** and ICN, (**2**·ICN)$_2$ is more stable than the CT and tbp **2**·ICN adducts by 1.20 and 3.64 kcal mol^{-1}, respectively. Contrarily, in all the hypervalent compounds of **2**

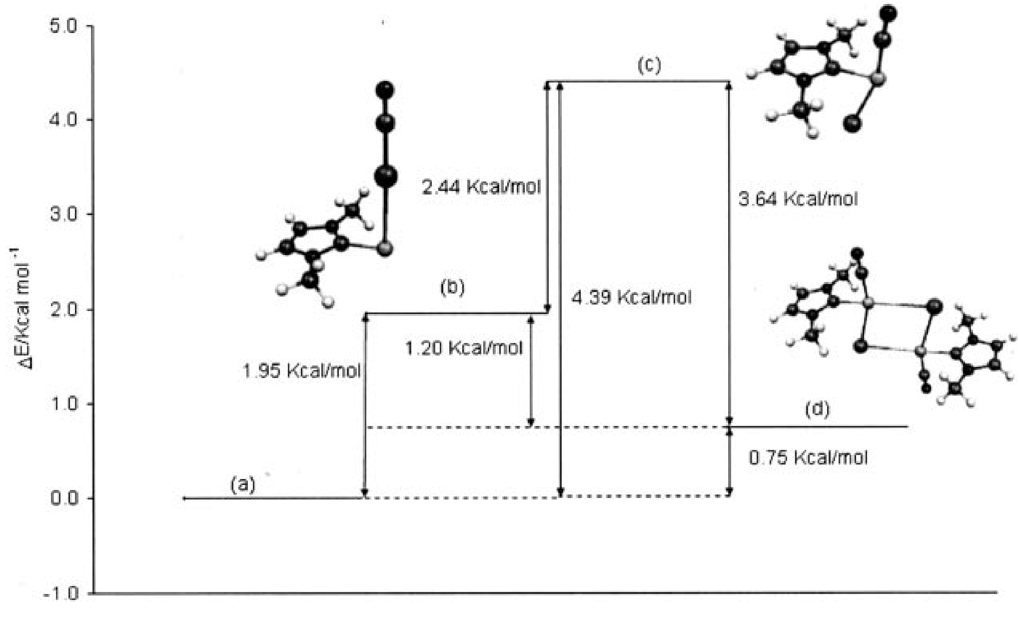

Figure 5. Relative DFT energies between CT and tbp adducts of **2** and ICN with respect to the free components: (a) ΔE[**2**+ICN]; (b) ΔE[**2**·ICN (CT)]; (c) ΔE[**2**·ICN (tbp)]; (d) 1/2 ΔE[(**2**·ICN)$_2$]

with halogens and inter-halogens, the T-shaped adduct formation always occurs with a stabilization energy >10.25 kcal mol^{-1}, which is the value calculated for **2**·I$_2$ (see values for all considered systems in the Theoretical Calculations section).

In this respect, we note that although very small changes are calculated in the I−Se−X system on passing from X = I to Br, and Cl, hypervalent selenium compounds with ICl are unknown. Thus, it should also be possible to prepare S- and Se-hypervalent tbp adducts with ICl, which are still unknown, despite numerous attempts to synthesize them. In fact, the Se-hypervalent system with ICl is expected to be very similar to that observed with IBr, as shown in Figure 4 by the regular trend and small variations in calculated Se−I distances and NBO charges on the iodine atom of I−Se−X systems (X = Cl, Br, I). This is strongly supported by the stabilization energy of the tbp **2**·ICl adduct, which is calculated as 16.70 kcal mol^{-1} with respect to the starting reagents **2** and ICl.

In conclusion, we report the first adduct between a selenium donor and ICN characterized by X-ray diffraction analysis. DFT calculations account for the strong polarity of the Se−I bond with the Se atom in a partial hypervalent state. **2**·ICN could also be described as the product of a donor−acceptor interaction between I$^-$ and the selenium atom of the organic cation [**2**·CN]$^+$. DFT calculations clarify the ability of the organic cation [**2**·CN]$^+$ to interact with I$^-$ donors in the two directions predetermined by the compositions of LUMO and LUMO+1, thus explaining the dimeric nature of **2**·ICN. The two different views lead to exactly the same final product: in the first case we consider the selenium partially hypervalent and a strong polarization of the Se···I bond (charge separation of 0.665e between the two fragments in **2**·ICN); in the second case, the ions approach until 0.335 electrons are reversed from I$^-$ into the LUMO of the cation.

Experimental Section

Materials and Methods: All solvents and reagents were purchased from Aldrich and used as received. Elemental analysis and FT-Raman spectra were carried out as described previously.[12]

Synthesis of 2·ICN: Compound **2**·ICN was obtained as brown crystals (60% yield) by slow evaporation in air at room temperature of a mixture of 1,3-dimethyl-4-imidazoline-2-selone (**2**) (50 mg, 0.286 mmol) and ICN in a 1:1 molar ratio in CH$_2$Cl$_2$. C$_6$H$_8$IN$_3$Se: calcd. C 21.97, H 2.46, N 12.81; found C 22.10, H 2.56, N 12.98. FT-IR (2500−500 cm^{-1}): $\tilde{\nu}$ = 2078 w, 1561 m, 1493 ms, 1417 mw, 1391 w, 1338 w, 1240 vs, 1159 m, 1091 m, 1023 m, 858 m, 771 s, 760 vs, 734 s, 649 s, 612 w. FT-Raman (500−100 cm^{-1}; relative intensities in parentheses related to the highest peak taken equal to 10): $\tilde{\nu}$ = 278(0.9), 258(2.6), 221(10), 195(8), 143(0.3).

X-ray Crystal Structure Determination of 2·ICN: 1834 diffraction data were collected on a Nonius CAD-4 diffractometer with graphite-monochromated Mo-K_α (λ = 0.71073 Å) radiation. The structure was solved by Patterson and Fourier methods and refined on F^2 using SHELXL-97.[17] Non-hydrogen atoms were refined with anisotropic thermal parameters. Hydrogen atoms were experimentally observed and allowed to ride on the pertinent atoms. C$_6$H$_8$IN$_3$Se, M = 328.01, triclinic, space group $P\bar{1}$ (No. 2), a = 6.946(1), b = 8.567(2), c = 8.907(2) Å; α = 98.54(1), β = 95.52(1), γ = 91.18(1)°; U = 521.4(1) Å^3, Z = 2, $d_{\mathrm{calcd.}}$ = 2.089 g·cm^{-3}, T = 293(2) K, μ(Mo-K_α) = 6.511 mm^{-1}, wR_2 = 0.077, R = 0.030 for 1593 observed reflections [$I > 2\sigma(I)$]. CCDC-205962 contains the supplementary crystallographic data for this paper. These data can be obtained free of charge at www.ccdc.cam.ac.uk/conts/retrieving.html [or from the Cambridge Crystallographic Data Centre, 12 Union Road, Cambridge CB2 1EZ, UK; Fax: (internat.) + 44-1223/336-033; E-mail: deposit@ccdc.cam.ac.uk].

Theoretical Calculations: Using the commercially available suite of programs in the Gaussian 98 package,[18] quantum-mechanical DFT-calculations on **2**, **2**·Br$_2$, **2**·I$_2$, **2**·IBr, [**2**·Br]$^+$, and [**2**·I]$^+$ have been reported.[11,12] For the present work, DFT-calculations were carried out on Cl$_2$, Br$_2$, I$_2$, IBr, ICl, ICN, **1**·BrCN, **2**·Cl$_2$, **2**·ICl, **2**·ICN (both CT and T-shaped), (**2**·ICN)$_2$, and [**2**·CN]$^+$ at the same level of theory as the previous calculations, i.e. using the hybrid Becke3LYP functional,[19] the Schäfer, Horn and Ahlrichs pVDZ[20] basis sets for C, H, N, O, S, and Se, and the LANL2DZ basis sets, together with effective core potentials (ECP)[21] for halogen atoms. For **2**·Br$_2$, the 6−31 g** basis set was used as described previously.[11] For comparison, the calculations on [**2**·CN]$^+$ were extended to the sulfured analogue [**1**·CN]$^+$. Numerical integration was performed using the FineGrid option, which indicates that a total of 7500 points are used for each atom, and the optimized structure was verified by normal-mode harmonic frequency analysis obtained using the second derivatives of the DFT energy, and computed by differentiation of the DFT energy gradients. For all compounds, zero-point energy corrections were applied to calculate the relative total energies. NBO calculations[15] were performed for each molecule using the converged density matrix corresponding to the equilibrium geometries. For all calculations, no basis set superposition error (BSSE) correction was applied. The results of the calculations were analyzed with the MOLEKEL 4.3[22] and Molden 3.9[23] programs. The ZPE corrected total energies of the selenium hypervalent adducts compared with the free components are: ΔE(**2**·Cl$_2$) = −33.01; ΔE(**2**·Br$_2$) = −28.95; ΔE(**2**·I$_2$) = −10.25; ΔE (**2**·ICl) = −16.70; ΔE (**2**·IBr) = −13.89; ΔE (**2**·ICN)$_{\mathrm{CT}}$ = +1.95; ΔE (**2**·ICN)$_{\mathrm{tbp}}$ = +4.39; 1/2ΔE[(**2**·ICN)$_2$] = +0.75 kcal·mol^{-1}. Calculations were performed on a SGI Origin 3800 with 128 RISC 14000 processor elements running at 500 MHz equipped with 128 Gb of DRAM.

Further Information: Optimized geometries in the form of Cartesian orthogonal coordinates, frontier orbital composition, NBO charges, and harmonic frequencies for each mentioned compound are available from the authors on request.

Acknowledgments

CINECA (Consorzio Interuniversitario per il Calcolo Automatico dell'Italia Nord Orientale) is gratefully acknowledged for computational facilities.

---

[1] R. J. Gillespie, I. Hargittai, *The VSEPR Model of Molecular Geometry*, Allyn and Bacon, **1991**, Boston, Massachusetts, USA.

[2] C. W. Perkins, J. C. Martin, A. J. Arduengo, W. Law, A. Alegria, J. K. Kochi, *J. Am. Chem. Soc.* **1980**, *102*, 7753−7759.

[3] Ky Akiba, *Chemistry of Hypervalent Compounds*, Wiley-VCH, **1999**, New York, USA.

[4] N. C. Baenziger, R. E. Buckles, R. J. Maner, T. D. Simpson, *J. Am. Chem. Soc.* **1969**, *91*, 5749−5755.

[5] W. Nakanishi, S. Hayashi, H. Tukada, H. Iwamura, *J. Phys. Org. Chem.* **1990**, *3*, 358−368.

[6] M. C. Aragoni, M. Arca, F. Demartin, F. A. Devillanova, A. Garau, F. Isaia, V. Lippolis, G. Verani, *Trends, Inorg. Chem.* **1999**, *6*, 1−18.

[7] F. Bigoli, A. M. Pellinghelli, P. Deplano, F. A. Devillanova, V. Lippolis, M. L. Mercuri, E. F. Trogu, *Gazz. Chim. It.* **1994**, *124*, 445−454.

[8] N. Kuhn, T. Kratz, G. Henkel, *Chem. Ber.* **1994**, *127*, 849−851.

[9] A. J. Arduengo, E. M. Burgess, *J. Am. Chem. Soc.* **1977**, *99*, 2376−2378.

[10] N. Bricklebank, P. J. Skabara, D. E. Hibbs, M. B. Hursthouse, K. M. Abdul Malik, *J. Chem. Soc., Dalton Trans.* **1999**, 3007−3014.

[11] M. C. Aragoni, M. Arca, A. J. Blake, F. A. Devillanova, W.-W. du Mont, A. Garau, F. Isaia, V. Lippolis, G. Verani, C. Wilson, *Angew. Chem. Int. Ed.* **2001**, *40*, 4229−4232.

[12] M. C. Aragoni, M. Arca, F. Demartin, F. A. Devillanova, A. Garau, F. Isaia, F. Lelj, V. Lippolis, G. Verani, *Chem. Eur. J.* **2001**, *7*, 3122−3133 and references cited therein.

[13] M. D. Rudd, S. V. Lindeman, S. Husebye, *Acta Chem. Scand.* **1997**, *51*, 689−708.

[14] F. Bigoli, P. Deplano, F. A. Devillanova, V. Lippolis, M. L. Mercuri, M. A. Pellinghelli, E. F. Trogu, *Eur. J. Inorg. Chem.* **1998**, 137.

[15] A. E. Reed, L. A. Curtiss, F. Weinhold, *Chem. Rev.* **1988**, *88*, 899−926.

[16] NBO charges on [**2**·ICN] and $[\mathbf{2}\cdot\mathrm{ICN}]_2$: C1 0.271, 0.280; N2/N3 −0.394, −0.394; C3/C4 −0.016, −0.019; Se 0.472, 0.488; I −0.665, −0.718; C8 −0.027, 0.005; N9 −0.351, −0.346. Mulliken charges on [**2**·ICN] and $[\mathbf{2}\cdot\mathrm{ICN}]_2$: C1 −0.278, −0.260; N2/N3 −0.142, −0.149; C3/C4 0.086, 0.085; Se 0.771, 0.810; I −0.560, −0.624; C8 −0.442, −0.429; N9 −0.117, −0.104 e.

[17] G. M. Sheldrick, SHELXL-97, University of Göttingen, **1997**.

[18] Gaussian 98, Revision A.7, M. J. Frisch, G. W. Trucks, H. B. Schlegel, G. E. Scuseria, M. A. Robb, J. R. Cheeseman, V. G. Zakrzewski, J. A. Montgomery, Jr., R. E. Stratmann, J. C. Burant, S. Dapprich, J. M. Millam, A. D. Daniels, K. N. Kudin, M. C. Strain, O. Farkas, J. Tomasi, V. Barone, M. Cossi, R. Cammi, B. Mennucci, C. Pomelli, C. Adamo, S. Clifford, J. Ochterski, G. A. Petersson, P. Y. Ayala, Q. Cui, K. Morokuma, D. K. Malick, A. D. Rabuck, K. Raghavachari, J. B. Foresman, J. Cioslowski, J. V. Ortiz, A. G. Baboul, B. B. Stefanov, G. Liu, A. Liashenko, P. Piskorz, I. Komaromi, R. Gomperts, R. L. Martin, D. J. Fox, T. Keith, M. A. Al-Laham, C. Y. Peng, A. Nanayakkara, C. Gonzalez, M. Challacombe, P. M. W. Gill, B. Johnson, W. Chen, M. W. Wong, J. L. Andres, C. Gonzalez, M. Head-Gordon, E. S. Replogle, J. A. Pople, Gaussian, Inc., Pittsburgh PA, **1998**.

[19] [19a] A. D. Becke, *J. Chem. Phys.* **1993**, *98*, 1372−1377; *J. Chem. Phys.* **1993**, *98*, 5648−5652. [19b] C. Lee, W. Yang, R. G. Parr, *Phys. Rev. B* **1988**, *37*, 785−789.

[20] A. Schäfer, H. Horn, R. Ahlrichs, *J. Chem. Phys.* **1992**, *97*, 2571−2577.

[21] P. J. Hay, W. R. Wadt, *J. Chem. Phys.* **1985**, *82*, 270−283.

[22] MOLEKEL 4.3, P. Flükiger, H. P. Lüthi, S. Portmann, and J. Weber, Swiss Center for Scientific Computing, Manno (Switzerland), **2000**.

[23] G. Schaftenaar, J. H. Noordik, *J. Comput.-Aided Mol. Design* **2000**, *14*, 123−134.

Received October 21, 2003
Early View Article